Critical behavior of $La_{1-x}Sr_xMnO_3$ ($0 \leqslant x \leqslant 0.35$) by thermal diffusivity measurements

A. Oleaga and A. Salazar
Departamento Física Aplicada I, Escuela Superior de Ingenieros, Universidad del País Vasco, Alameda Urquijo s/n 48013-Bilbao, Spain

D. Prabhakaran and A. T. Boothroyd
Departments of Physics, Clarendon Laboratory, University of Oxford, Oxford OX1 3PU, United Kingdom
(Received 8 March 2004; published 2 November 2004)

An ac photopyroelectric calorimeter has been used to measure the thermal diffusivity of the perovskite manganite family $La_{1-x}Sr_xMnO_3$ on a set of single crystals with doping range $0 \leqslant x \leqslant 0.35$. Taking into account that the inverse of the thermal diffusivity has the same critical behavior as the specific heat, the critical exponent α of the magnetic transitions has been obtained. The results point to short-range interaction models for pure magnetic transitions. In the pure and lightly doped samples ($x < 0.10$), where the transition is antiferromagnetic-paramagnetic, the critical exponent is consistent with the Heisenberg model ($\alpha = -0.11$). For the highly doped samples ($x > 0.28$), where there is a pure ferromagnetic-paramagnetic transition, the critical exponent is exactly that of an Ising behavior ($\alpha = +0.11$). For $0.10 \leqslant x < 0.28$ no universality class was found and this behavior has been discussed taking into account the complexity of the phase diagram in this concentration range.

DOI: 10.1103/PhysRevB.70.184402 PACS number(s): 75.40.−s, 64.60.Fr, 65.40.−b, 75.30.Kz

I. INTRODUCTION

Perovskite manganites $L_{1-x}A_xMnO_3$ (L = lanthanide, A = alkaline earth) have attracted great attention in the last years due to their colossal magnetoresistance.[1,2] The large variation in the carrier mobility originates from an insulator-metal transition that is closely associated with the magnetic ordering. Among these oxides, $La_{1-x}Sr_xMnO_3$ is specially interesting due to the fact that its Curie temperature in the concentration range where colossal magnetoresistance takes place is the highest one. In Fig. 1, a schematic phase diagram mainly showing the magnetic and metallic-insulator transitions has been drawn after Urushibara *et al.*[3] and Zhou and Goodenough.[4] It is clear from this diagram that the electrical and magnetic properties of pure $LaMnO_3$ change strongly with strontium doping, which introduces holes in the manganese e_g band, eventually producing mobile holes and conduction. The low temperature phase for the pure and lightly doped samples ($x < 0.10$) is antiferromagnetic insulator, becoming a ferromagnetic insulator in the range $0.10 \leqslant x < 0.16$, above which the insulator character changes to metallic. The change in magnetic behavior has been qualitatively explained by the double exchange hopping mechanism[5–7] in which the antiferromagnetic phase is progressively destroyed by the ferromagnetic coupling induced by the hopping of the e_g electron from a Mn^{3+} ion in the corresponding hole of a neighboring Mn^{4+}. Regarding the high-temperature phase, this is a paramagnetic insulator up to about $x = 0.28$, becoming metallic from then on.

In order to understand the mechanisms of the colossal magnetoresistance, much work has been devoted to the study of the electrical and magnetic properties, taking into account the strong interplay of magnetism, electron-lattice coupling, and orbital and charge ordering in these materials. However, the change in the physical properties as Sr concentration is increased, as well as the details of the physical mechanisms responsible for the different transitions, are not yet well understood. Besides, there are no systematic studies of the critical behavior made on a set of high-quality single crystals grown in the same laboratory, with the same conditions and with a broad range of strontium concentrations so as to be able to compare with certainty the results obtained. Concerning the magnetic transitions, one way of clarifying its nature is the determination of the critical exponents associated with them. In this particular, there is much controversy so as to whether long-range or short-range interactions are at the root of the physical properties these materials show.

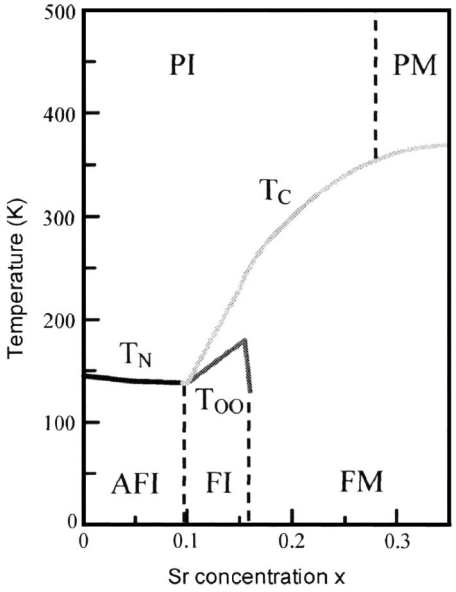

FIG. 1. Schematic phase diagram for $La_{1-x}Sr_xMnO_3$: P stands for paramagnetic, F for ferromagnetic, AF for antiferromagnetic, I for insulator, M for metallic, T_{OO} for orbital-ordering temperature, and T_N and T_C stand for the Néel and Curie temperatures.

TABLE I. Theoretical values of the critical exponents (Ref. 18).

Model	β	γ	δ	α	A^+/A^-
Mean field	0.5	1.0	3.0	0	
3D *XY*	0.333	1.34		−0.007	1.03
3D Heisenberg	0.365	1.39	4.80	−0.115	1.521
3D Ising	0.325	1.24	4.82	+0.11	0.524

In the last years several papers dealing with the critical exponents of $La_{1-x}Sr_xMnO_3$ have been published.[8–17] However, the results are not conclusive and sometimes they are contradictory. In Table I the theoretical values of the critical exponents for the main models for three-dimensional (3D) magnets are shown. There β, γ, δ, and α are the critical exponents of the magnetization, susceptibility, critical isotherm, and specific heat, respectively. The mean field model implies long-range interactions between ions while the rest are founded on short-range models. Within this group the 3D Heisenberg model applies for isotropic ferromagnets and the 3D Ising model for anisotropic ones. In the case of the antiferromagnetic parent compound, $LaMnO_3$, there is a general agreement that it belongs to the 3D Heisenberg universality class. However, as far as we are concerned, there are no measurements of the critical parameters exactly confirming this model. In this way, Moussa *et al.*[8] obtained $\beta=0.28$, quite below the 3D Heisenberg model, and Cestelli *et al.*,[9] while obtaining $\beta=0.36$ (perfect Heisenberg), concluded from their results on muon spin relaxation that there is a crossover to Ising behavior due to anisotropy. In the ferromagnetic insulator range, the sample doped with $x=0.125$ has been studied by Nair *et al.*,[10] giving β and γ values corresponding to a Heisenberg model. Concerning the measurements on ferromagnetic metallic samples ($0.20 \leqslant x \leqslant 0.30$), there is a wide dispersion in the results and in the conclusions. On the one hand, Mohan *et al.*,[11] Schwarz *et al.*,[12] and Lofland *et al.*,[13] performing different magnetic measurements, agree on the validity of the mean field model for the material, which means long-range order. On the other hand, there are works that support the short-range models, either Heisenberg or Ising. Vasiliu and Lynn[14] obtained $\beta=0.30$ which stands for the Heisenberg model, while Kim *et al.*[15] and Lin *et al.*,[16] through specific heat and magnetic measurements, obtained results closer to the Ising model. Gosh *et al.*[17] obtained a β value, in agreement with a Heisenberg model but a γ value in disagreement.

The differences in the measurements may be due to the quality of the samples, to their being single or polycrystalline, to the composition control or to the fitting range. One of the problems while interpreting the results is that the theoretical β and γ values for the different models are not so different so as to be the best discriminators. From Table I it can be seen that the most promising critical parameter is the one derived from the specific heat α because its value and its sign change from one model to another. Besides, it is accompanied by the coefficients A^+, A^-, whose ratio and signs also depend on the model. Taking into account the relationship between specific heat c and thermal diffusivity D through the equation $c=K/\rho D$ (where ρ stands for density and K for thermal conductivity), the inverse of the thermal diffusivity has the same critical behavior as the specific heat, provided that the thermal conductivity does not present singularities at the magnetic transitions. Thermal conductivity measurements performed by Zhou and Goodenough[4] and Fujishiro and Ikebe[19] have shown that there is no such singularity in lanthanum-strontium manganites.

The purpose of this work is to study the dependence of the critical parameter α on Sr concentration through the measurement of the thermal diffusivity D of a set of single crystals with Sr concentration ranging from 0 to 0.35, trying to elucidate which models are applicable in both the antiferromagnetic-paramagnetic and ferromagnetic-paramagnetic transitions.

II. SAMPLES AND EXPERIMENTAL TECHNIQUES

Single crystals of $La_{1-x}Sr_xMnO_3$ ($x=0$, 0.05, 0.10, 0.125, 0.15, 0.165, 0.20, 0.25, 0.30, and 0.35) were grown by the floating-zone technique. The polycrystalline seeds were prepared from a stoichiometric mixture of La_2O_3, $SrCO_3$, and MnO_2 calcined and sintered at 1200 °C for 72 h. Crystals were grown in an Ar-rich atmosphere at a pressure of 6–8 atm. in order to reduce manganese evaporation. The nature of the crystal surface was checked by optical and scanning electron microscopy, while x-ray powder and Laue diffraction was used to assess the phase purity, structure, and crystalline quality. Surface images of polished cross sections of the crystals are smooth, with no evidence of microcracks, segregation, or twin boundaries. In the case of the sample $x=0.35$ it has not been possible to obtain a perfect single crystal but it contains a few grains. Detailed growing procedures were reported elsewhere.[20] Slices of thickness between 0.3 and 0.4 mm were cut from the grown rods, perpendicular to the growth direction (c axis) for this study.

Thermal diffusivity measurements have been performed by a high-resolution ac photopyroelectric calorimeter in the standard back detection configuration.[21,22] A mechanically modulated He-Ne laser beam of 5 mW illuminates the upper surface of the sample under study. Its rear surface is in thermal contact with a 350-μm-thick $LiTaO_3$ pyroelectric detector with Ni-Cr electrodes on both faces, by using an extremely thin layer of a high heat-conductive silicone grease (Dow Corning, 340 Heat Sink Compound). The photopyroelectric signal is processed by a lock-in amplifier in the current mode. Both sample and detector are placed inside a nitrogen bath cryostat that allows measurements in the temperature range from 77 to 500 K, at rates that vary from 100 mK/min for measurements on a wide temperature range to 10 mK/min for high resolution runs close to the phase transitions. If the sample is opaque and thermally thick (i.e., its thickness ℓ is higher than the thermal diffusion length $\mu=\sqrt{D/\pi f}$) the natural logarithm and the phase of the normalized photopyroelectric voltage at a fixed temperature have a linear dependence on $\sqrt{f}$, with the same slope m, from which the thermal diffusivity of the sample can be measured,[21,22]

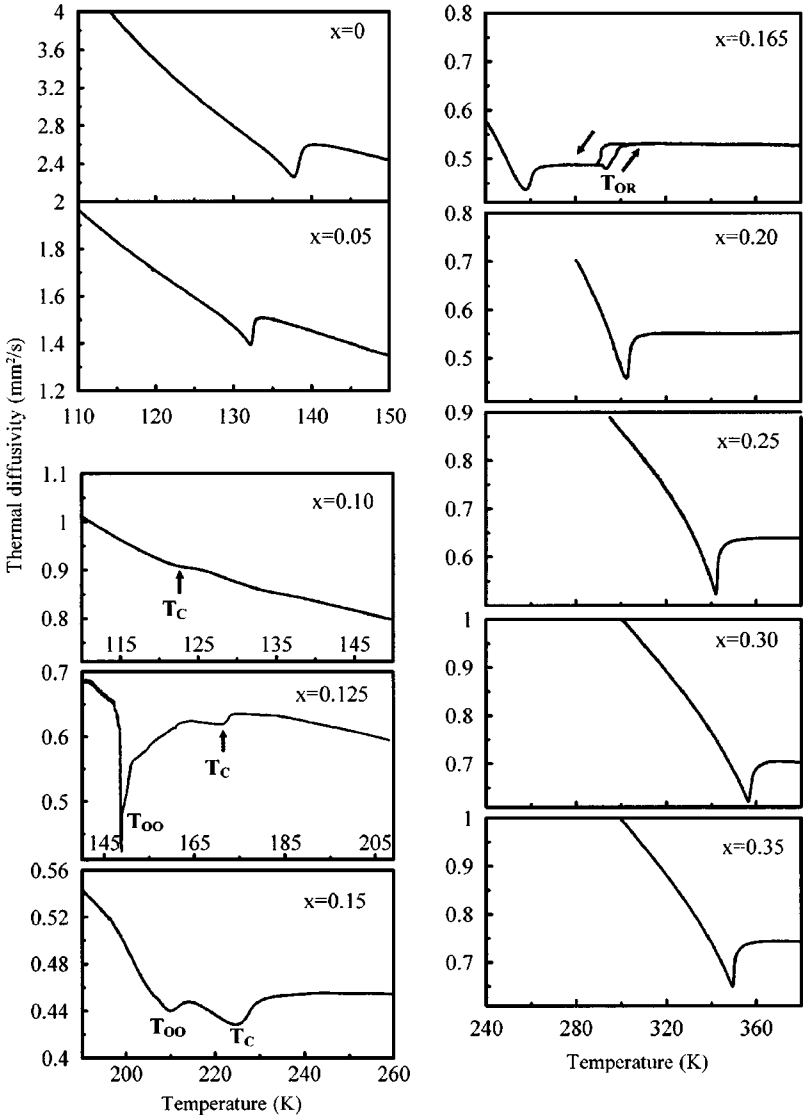

FIG. 2. Temperature dependence of the thermal diffusivity for the samples $0 \leqslant x \leqslant 0.35$ showing the magnetic transitions. The dips in diffusivity signal the Néel ($x=0, 0.05$), or Curie temperature. Other transitions present in the temperature ranges shown are marked: orbital-ordering for $x=0.125$, 0.15 (T_{OO}) and structural for $x=0.165$ (T_{OR}).

$$D = \frac{\ell^2 \pi}{m^2}. \tag{1}$$

Once the thermal diffusivity has been measured at a certain reference temperature (D_{ref}), the temperature is changed while recording the phase of the photopyroelectric signal. Defining the phase difference as $\Delta(T)$, the temperature dependence of the thermal diffusivity is given by[23,24]

$$D(T) = \left[\frac{1}{\sqrt{D_{\text{ref}}}} - \frac{\Delta(T)}{\ell \sqrt{\pi f}} \right]^{-2}. \tag{2}$$

This technique is specially suited for the measurement of the through-thickness thermal diffusivity around phase transitions, since small temperature gradients in the sample produce a good signal-to-noise ratio, letting thermal diffusivity be measured with high accuracy.

III. EXPERIMENTAL RESULTS AND FITTING PROCEDURES

Thermal diffusivity has been measured for all the samples as a function of temperature in the region around the magnetic transitions. The results in a wide temperature range are shown in Fig. 2. In all cases a dip defines the critical temperature but, as can be seen from the figures, the shape is quite different depending on the samples. While for the undoped sample there is a sharp and narrow dip, the sharpness is reduced as x increases and disappears for $x=0.10$, where the ferromagnetic behavior has begun. For $x=0.125$ the magnetic transition is signaled by a small change in diffusivity. Then, as x is further increased the magnetic dips get a better definition and the rounding is progressively reduced. Note that there is a small anomaly in the value of the Curie temperature for the sample $x=0.35$, which, according to the phase diagram, should be higher than that of $x=0.30$. As has been mentioned in the preceding section, the sample $x=0.35$ is not a single crystal as the rest, but it contains few grains. The exact position of T_C depends on the quality of the crystal, as the dispersion of results among different authors using different crystals reveal. On the other hand, for some concentrations other transitions that are close to the magnetic one are also included. For the samples with $x=0.125$ and $x=0.15$ there is an orbital-ordering transition (T_{OO}) taking place just below T_C and for $x=0.165$ a first-order

orthorhombic-rhombohedral structural transition is signaled by a rising step in thermal diffusivity. These structural transitions, as well as the general changes in the value of the thermal diffusivity in these samples, have been discussed elsewhere.[25]

It is worth emphasizing that the variations in the shape of the peaks depend on the intrinsic characteristics of every sample, and not on differences on crystal quality. Besides, the rounding in the peaks can not be attributed to the experimental setup, because we have performed thermal diffusivity measurements on simple oxides (e.g., Cr_2O_3) obtaining far sharper, very well defined dips.[25] As the complexity of the matrix grows (which is the case for double oxides as $LaMnO_3$ and still more doping it with Sr) the rounding affects to broader regions, even if the samples are high quality single crystals.

To obtain the critical parameters, detailed measurements of the thermal diffusivity have been performed in the near vicinity of the Néel (T_N) or Curie (T_C) temperature in order to have very well defined curves. Then, the inverse of thermal diffusivity D has been fitted to the same function that is generally used for the specific heat,[26,27]

$$1/D = B + \overline{C}t + A|t|^{-\alpha}(1 + E|t|^{0.5}), \tag{3}$$

where $t=(T-T_C)/T_C$ is the reduced temperature and A, B, $\overline{C}$, and E are adjustable parameters for $T>T_C$. A similar equation is used for $T<T_C$ with prime parameters. The linear term represents a regular contribution to the inverse of diffusivity due to the transition itself, which means that $\overline{C}=\overline{C}'$. Continuity imposes that $B=B'$. The term $(1+E|t|^{0.5})$ is the well-known correction to scaling term. Following Marinelli and co-workers,[27] in order to reduce the statistical correlation among set of parameters, the expressions used for our fittings were

$$1/D = B + C(T - T_C) + A^+|T - T_C|^{-\alpha}(1 + E^+|T - T_C|^{0.5}), \quad t > 0 \tag{4a}$$

$$1/D = B + C(T - T_C) + A^-|T - T_C|^{-\alpha}(1 + E^-|T - T_C|^{0.5}), \quad t < 0. \tag{4b}$$

Provided that we consider $|T-T_C|$ as $|(T-T_C)/1\ K|$, parameters in Eqs. (3) and (4) have the same units; therefore, the same relations which apply among the parameters in Eq. (3) hold for Eqs. (4).

The data were simultaneously fitted for $T>T_C$ and $T<T_C$ with a nonlinear least square routine. First of all, we selected a fitting range close to the peak while avoiding the rounding, and kept fixed the value of T_C. We obtained a first fitting without the correction to scaling term and obtained a set of adjusted parameters. Then we let T_C vary and the data were fitted again. Afterwards, we tried to increase the number of points included in the fitting, first fixing t_{min} and increasing t_{max}, and then fixing t_{max} and decreasing $t$min. The last step was introducing the correction to scaling term trying to improve the fitting. In the whole process, we focused our attention on the rms deviations as well as on the deviation plots, which are the plots of the difference between the fitted values and the measured ones as a function of the reduced temperature.

The results of the fittings are presented in Table II and Fig. 3. They are all quite good fittings, as can be seen in the χ^2 values, in the parameter errors, as well as by the small visual deviation of the fitted functions with respect to the experimental ones. In the case of the samples in the range $0.10 \leqslant x \leqslant 0.165$, either the peak is not well defined or the rounding is too pronounced in order to perform any fitting.

IV. DISCUSSION AND CONCLUSIONS

The physical properties of the manganite family $La_{1-x}Sr_xMnO_3$ depend heavily on the degree of strontium doping and this is reflected on the fitting results. For the pure and lightly doped samples, in which the low-temperature phase is antiferromagnetic ($x<0.10$), the value and sign of the critical parameter α point directly to a 3D Heisenberg model, though the values are a bit lower than the theoretical one ($\alpha=-0.09$ for the pure sample and $\alpha=-0.08$ for $x=0.05$). This may be accounted for if there is some degree of anisotropy which makes the material deviate from the perfect Heisenberg behavior. Actually, the magnetic moments in the pure material are oriented along the b axis.[8,28] This source of anisotropy has been taken into account by Moussa *et al.*[8] in the undoped sample introducing a single ion anisotropic term in the Hamiltonian, through which they were able to explain their experimental β value, which was lower than expected within the framework of the pure Heisenberg model. They concluded that the strength of this anisotropic term is an order of magnitude lower than the regular terms in the Heisenberg Hamiltonian, leading to a reduction of the experimental critical values. Besides, the fact that the Heisenberg model nearly holds for both antiferromagnetic samples is in accordance with the Harris criterion,[29] which states that if $\alpha<0$ in a pure system, small disorder does not change the critical behavior. On the other hand, the experimental ratio A^+/A^- in both samples is close to 1 instead of to the theoretical 1.5, indicating again a deviation from the pure Heisenberg behavior.

In the ferromagnetic samples three regions can be distinguished. For $x>0.28$ the transition is purely magnetic and the critical parameter obtained for the two samples we have measured ($x=0.30$ and 0.35) is $\alpha=+0.11$, exactly the value predicted by the 3D Ising model. Although the ratio of the coefficients A^+/A^- does not reach the theoretical value (0.5), it tends to be closer to it as strontium concentration is increased (0.81, 0.74 for $x=0.30$, 0.35 respectively). These results mean that the 3D Ising model is applicable in this case, showing that short-range interaction models suitably describe the magnetic transitions in these manganites. In homogeneous magnets, the universality class of the magnetic phase transition depends on the range of the magnetic interaction $J(r)$.[30] The Heisenberg model is valid for isotropic 3D ferromagnets if $J(r)$ decreases with distance r faster than r^{-5}; on the other hand, the mean-field model is applicable if the dependence is slower than $r^{-4.5}$. In the double exchange model, effective ferromagnetic interaction is induced by the kinetics of electrons which favor extended states with ferro-

TABLE II. Results of the fitting for the six samples, including the critical exponent, range of the fitting, adjustable parameters, and deviation coefficient.

	$x=0$	$x=0.05$	$x=0.2$	$x=0.25$	$x=0.3$	$x=0.35$
α	-0.09 ± 0.01	-0.08 ± 0.008	$+0.32\pm0.06$	$+0.21\pm0.01$	$+0.11\pm0.01$	$+0.11\pm0.004$
A^+/A^-	1.02	0.97	1.52	0.99	0.81	0.74
$t_{min}-t_{max}(T<T_C)$	$9.5\times10^{-3}-3\times10^{-2}$	$4.9\times10^{-3}-1.9\times10^{-2}$	$9.7\times10^{-3}-2.4\times10^{-2}$	$5.3\times10^{-3}-1.8\times10^{-2}$	$6.4\times10^{-3}-1.7\times10^{-2}$	$7.4\times10^{-3}-1.7\times10^{-2}$
$t_{min}-t_{max}(T>T_C)$	$2.9\times10^{-3}-2.5\times10^{-2}$	$1.9\times10^{-3}-1.4\times10^{-2}$	$4.5\times10^{-3}-1.8\times10^{-2}$	$8.7\times10^{-4}-1.1\times10^{-2}$	$1.4\times10^{-3}-1\times10^{-2}$	$1.4\times10^{-3}-1\times10^{-2}$
A^+ (s/mm^2)	-0.43 ± 0.05	-0.55 ± 0.06	0.35 ± 0.09	0.44 ± 0.04	0.59 ± 0.06	0.376 ± 0.004
B (s/mm^2)	0.80 ± 0.05	1.18 ± 0.06	2.2 ± 0.4	1.35 ± 0.05	0.92 ± 0.06	1.052 ± 0.006
C (s/mm^2)	0.0189 ± 0.0005	0.0367 ± 0.0009	0.034 ± 0.002	0.0317 ± 0.0006	0.0050 ± 0.0001	0.0124 ± 0.0003
E^+	0.005 ± 0.002	0.040 ± 0.006	-1.6 ± 1.1	-0.27 ± 0.05	-0.0003 ± 0.0007	-0.078 ± 0.006
E^-	-0.14 ± 0.02	-0.19 ± 0.02	-0.8 ± 1.4	0.29 ± 0.02	0.0010 ± 0.0005	0.034 ± 0.002
χ^2	2.1×10^{-7}	1×10^{-7}	3.8×10^{-6}	5×10^{-6}	3.5×10^{-6}	1.6×10^{-6}

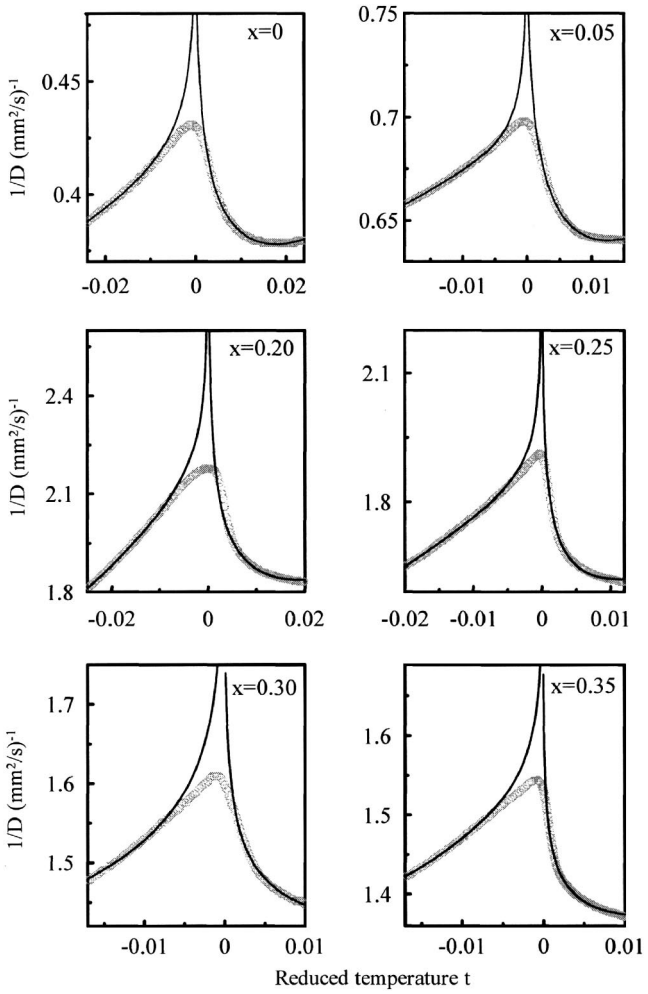

FIG. 3. Inverse of the thermal diffusivity as a function of the reduced temperature for $x=0$, 0.05, 0.20, 0.25, 0.30, and 0.35. Experimental curve (points) and fitted curve (full line). Not all experimental points are shown, in order to visually discriminate the quality of the fits.

magnetic spin background to gain the kinetic energy; thus, a long-range model would be expected to be of application. Nevertheless, in a recent study on manganites, Furukawa and Motome have showed, employing the moment-expansion Monte Carlo method,[31] that the universality class of the ferromagnetic transition driven only by a double exchange mechanism is consistent with that of short-range models instead of long-range ones. Our results for $x=0.30$ and 0.35 are indeed consistent with a short-range model, but with the 3D Ising instead of a 3D Heisenberg model, which suggests the presence of a large anisotropy at these compositions.

It is worth noticing that this Ising-like behavior has been previoulsy reported for $x>0.28$ (Refs. 16 and 17) and in another case the exponents obtained also agree with this model though they were atributed to a Heisenberg model.[14] Nevertheless, there is no complete agreement since Heisenberg and mean-field models have also been claimed to be of application.[13,17]

The second ferromagnetic region corresponds to the range $0.16<x<0.28$ where the characteristic feature is that, to-

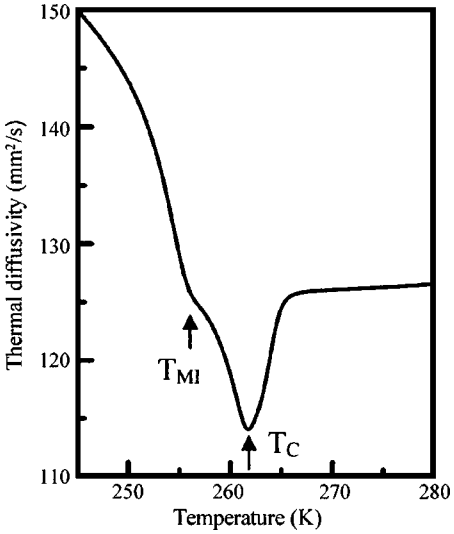

FIG. 4. Thermal diffusivity as a function of temperature for $La_{0.7}Ca_{0.3}MnO_3$ showing two transitions: metallic-insulator and ferromagnetic-paramagnetic.

gether with the ferromagnetic-paramagnetic transition, there is also a metallic-insulator transition at the same temperature. For the samples in which it has been possible to perform a fitting ($x=0.20$ and 0.25), there is no agreement with any universality class, though there is a tendency in the value and signs of the critical parameter α to a 3D Ising model. As it can be seen from Table II, starting from $x=0.20$ and increasing the strontium concentration, both α and the ratio A^+/A^- are reduced till an Ising-like behavior is revealed in the region previously described. The deviation from universality in these samples can be explained by the fact that the transition is not purely magnetic. Since the electrical properties vary at the same time, the shape of the thermal diffusivity dip should be modified with respect to a pure magnetic transition and therefore the fitting and the values of the critical exponents should be altered. As an example of how thermal diffusivity is affected by the presence of two transitions, measurements performed on $La_{0.7}Ca_{0.3}MnO_3$ are shown in Fig. 4. In this sample magnetic and electric transitions are close to one another (but not superimposed), showing characteristic features in thermal diffusivity: the elbow at low temperature corresponds to the metallic-insulator transition and the dip signals the Curie temperature. It is expected that the magnetic dip be affected when both transitions take place at the same temperature, thus modifying the critical behavior.

The third ferromagnetic region is that within the range $0.10 \leqslant x < 0.16$, which is the transition region from the superexchange-dominated antiferromagnetic manganites to the double exchange driven ferromagnetic manganites. As before, the ferromagnetic-paramagnetic transition is also a metallic-insulator transition; but now, below and very close to T_C, there is an orbital-ordering transition superimposed to an insulator-metallic change (see Fig. 1). In between there is a peculiar phase where dynamic segregation into hole-rich and hole-poor phases has been reported,[32] leading to a spin glass phase in low magnetic fields, which is transformed into a ferromagnetic vibronic phase if higher fields are applied.[33] The nearly null dip obtained in our measurements of thermal diffusivity at T_C for $x=0.10$ and the gradual rising of the transition features as x is increased (see Fig. 2) are analogous to the behavior observed by Liu *et al.* on specific heat measurements.[33] The extraordinary complexity of the physical interactions that take place in this region must be responsible for the almost extinction of the D dip, specially for the case of $x=0.10$ where nearly everything happens at the same temperature.

In conclusion, we have performed high-resolution thermal diffusivity measurements on single crystals $La_{1-x}Sr_xMnO_3$ ($0 \leqslant x \leqslant 0.35$) in the vicinity of the magnetic transitions. From the fitting of the inverse of the diffusivity, the critical parameter α has been obtained. The results agree with short-range coupling models for pure magnetic transitions. In the case of the antiferromagnetic-paramagnetic transitions ($x<0.10$) the data fit to a 3D Heisenberg model, while for the ferromagnetic-paramagnetic samples with $x>0.28$ the data fit to a 3D Ising model, which implies the presence of magnetic anisotropy. For the range $0.10 \leqslant x < 0.28$, where the transition is not purely magnetic, no universal behavior was found.

[1] M.B. Salamon and M. Jaime, Rev. Mod. Phys. **73**, 583 (2001).
[2] E. Dagotto, T. Hotta, and A. Moreo, Phys. Rep. **344**, 1 (2001).
[3] A. Urushibara, Y. Moritomo, T. Arima, A. Asamitsu, G. Kidon, and Y. Tokura, Phys. Rev. B **51**, 14103 (1995).
[4] J. S. Zhou and J.B. Goodenough, Phys. Rev. B **64**, 024421 (2001).
[5] C. Zener, Phys. Rev. **82**, 403 (1951).
[6] P.W. Anderson and H. Hasegawa, Phys. Rev. **100**, 675 (1955).
[7] P.G. de Gennes, Phys. Rev. **100**, 564 (1955).
[8] F. Moussa, M. Hennion, J. Rodriguez-Carvajal, H. Moudden, L. Pinsard, and A. Revcolevschi, Phys. Rev. B **54**, 15149 (1996).
[9] M. Cestelli Guidi, G. Allodi, R. De Renzi, G. Guidi, M. Hennion, L. Pinsard, and A. Amato, Phys. Rev. B **64**, 064414 (2001).
[10] S. Nair, A. Banerjee, A.V. Narlikar, D. Prabhakaran, and A.T. Boothroyd, Phys. Rev. B **68**, 132404 (2003).
[11] Ch. V. Mohan, M. Seeger, H. Kronmüller, P. Murugaraj, and J. Maier, J. Magn. Magn. Mater. **183**, 348 (1998).
[12] A. Schwartz, M. Scheffler, and S.M. Anlage, Phys. Rev. B **61**, R870 (2000).
[13] S.E. Lofland, V. Ray, P.H. Kim, S.M. Bhagat, M.A. Manheimer, and S.D. Tyagi, Phys. Rev. B **55**, 2749 (1997).
[14] L. Vasiliu-Doloc and J.W. Lynn, J. Appl. Phys. **83**, 7342 (1998).
[15] D. Kim, B.L. Zink, F. Hellman, and J.M.D. Coey, Phys. Rev. B **65**, 214421 (2002).
[16] P. Lin, S.H. Chun, M.B. Salamon, Y. Tomioka, and Y. Tokura, J. Appl. Phys. **87**, 5825 (2000).
[17] K. Gosh, C.J. Lobb, R.L. Greene, S.G. Karabashev, D.A. Shulyatev, A.A. Arsenov, and Y. Mukovskii, Phys. Rev. Lett. **81**,

4740 (1998).
[18] H.E. Stanley, *Introduction to Phase Transitions and Critical Phenomena* (Oxford University Press, New York, 1971).
[19] H. Fujishiro and M. Ikebe, Physica B **263–264**, 691 (1999).
[20] D. Prabhakaran, A.I. Coldea, A.T. Boothroyd, and S.J. Blundell, J. Cryst. Growth **237–239**, 806 (2002).
[21] M. Marinelli, U. Zammit, F. Mercuri, and R. Pizzoferrato, J. Appl. Phys. **72**, 1096 (1992).
[22] M. Chirtoc, D. Dadarlat, D. Bicanic, J.S. Antoniow, and M. Egée, in *Progress in Photothermal and Photoacoustic Science and Technology*, edited by A. Mandelis and P. Hess (SPIE, Bellingham, Washington, 1997), Vol. 3.
[23] S. Delenclos, M. Chirtoc, A. Hadj Sahraoui, C. Kolinsky, and J.M. Buisine, Rev. Sci. Instrum. **73**, 2773 (2002).
[24] A. Salazar, Rev. Sci. Instrum. **74**, 825 (2003).
[25] A. Salazar, A. Oleaga, and D. Prabhakaran, Int. J. Thermophys. **25**, 1269 (2004).
[26] A. Kornblit and G. Ahlers, Phys. Rev. B **11**, 2678 (1975).
[27] M. Marinelli, F. Mercuri, U. Zammit, R. Pizzoferrato, F. Scudieri, and D. Dadarlat, Phys. Rev. B **49**, 9523 (1994).
[28] J.M.D. Coey, M. Viret, and S. von Molnar, Adv. Phys. **48**, 167 (1999).
[29] A.B. Harris, J. Phys. C **7**, 1671 (1974).
[30] M.E. Fisher, S. Ma, and B.G. Nickel, Phys. Rev. Lett. **29**, 917 (1972).
[31] N. Furukawa and Y. Motome, Appl. Phys. A: Mater. Sci. Process. **74**, S1728 (2002).
[32] J.S. Zhou, J.B. Goodenough, A. Asamitsu, and Y. Tokura, Phys. Rev. Lett. **79**, 3234 (1997).
[33] G.L. Liu, J.S. Zhou, and J.B. Goodenough, Phys. Rev. B **64**, 144414 (2001).